JOURNAL OF MATERIALS SCIENCE **39** (2004) 1397– 1401

Structural change of hydrothermal $BaTiO_3$ powder

J. H. LEE, H. H. NERSISYAN, H. H. LEE, C. W. WON
Rapidly Solidified Materials Research Center (RASOM), Chungnam National University, Yuseong, Daejeon 305-764, Korea; Korea Research Institute of Chemical Technology, P.O. 107, Yuseong, Daejeon 305-600, Korea
E-mail: jong-lee@cnu.ac.kr

Formation rate of tetragonal $BaTiO_3$ powder by hydrothermal synthesis and its dielectric property were studied. Submicron tetragonal $BaTiO_3$ powders were prepared hydrothermally, using $Ba(OH)_2{\cdot}8H_2O$, TiO_2 (anatase) and KOH as starting chemicals. Characterization via X-ray diffractometry, Field Emission Scanning Electron Microscopy confirmed that increasing calcination temperature (from 1100 to 1300°C) promotes the formation of tetragonal $BaTiO_3$. Tetragonal $BaTiO_3$ ceramics obtained from optimum condition (Tetragonal $BaTiO_3$ powders calcined at 1200°C for 3 h after hydrothermal synthesized at 200°C for 168 h) exhibited submicron size of 0.5–0.7 μm, monodispersed type and high relative permittivity.

1. Introduction

Tetragonal $BaTiO_3$ has excellent dielectric properties, which makes it the most important ferroelectric material used in the manufacture of thermistors, ceramic capacitors and especially multilayer ceramic capacitors (MLCCs) [1]. The performances of MLCCs are enhanced by decreasing the layer thickness of ferroelectric material and this has been realized by decreasing particle size. Hence, recent emphasis has focused on chemical methods such as wet precipitation which allows the formation of a much smaller particle size compared to solid state synthesis [2–5]. However, for the most precipitation processes, the product is either an amorphous phase or a precursor compound so that a calcination step at 800–1000°C, followed by milling, is usually required to form a crystalline $BaTiO_3$ powder.

Hydrothermal synthesis provides an alternative route for the formation of crystalline oxide powders directly in very basic water and normally at a relatively low temperature <300°C. Hydrothermal $BaTiO_3$ powders typically have fine particle sizes in the range of 50–400 nm and a narrow distribution of sizes making these powders highly sinterable. There are a number of new structural characteristics in hydrothermal $BaTiO_3$ powders that are not observed for powders prepared by conventional solid state reaction at higher temperature. The literature indicates that hydrothermal synthesis methods result in a cubic-like structure and the unique structural characteristics are attributed to the small crystallite size, defects in the crystallite and/or the presence of a surface layer [6]. However tetragonality in the $BaTiO_3$ powder is favorable in order to enhance the dielectric properties after sintering. Hence, the hydrothermal synthesis and characterization of tetragonal $BaTiO_3$ powder have been extensively investigated by many investigators. It has been reported that the formation reaction of tetragonal $BaTiO_3$ powder via moderate hydrothermal conditions takes place over several days [7], while cubic phase is obtained within several hours [5, 8]. From the previous results, the reaction mechanism of tetragonal $BaTiO_3$ phase seems to be somewhat different from the cubic known as dissolution and precipitation.

In this study, the experimental results on the hydrothermal synthesis of tetragonal $BaTiO_3$ powders have been obtained and the formation mechanism of tetragonal phase under hydrothermal conditions has also been tentatively proposed.

2. Experimental procedure

$Ba(OH)_2{\cdot}8H_2O$ and TiO_2 (anatase, 98%) were used as the barium and titanium sources, respectively. KOH (95%) was used as an alkaline mineralizer. The system was purged with argon, sealed and heated rapidly to the reaction temperature and held for given times. After the reaction, the product was washed with deionized water. The powder was dried in an oven for 24 h at 85°C. The morphology and size of the powders were observed in a field emission scanning electron microscope (FESEM) and crystal structure was analyzed by X-ray diffractometry. If a $BaTiO_3$ consists of equal volume fraction of a and c domains, the intensity of (200) peak is three times as much as that of (002) peak, hence the degree of tetragonality was estimated from the XRD 2θ scan spectra by comparing the intensities of (002) and (200) diffraction peaks originated from a and c domains, respectively. The degree of tetragonality, α was calculated as follows [9];

$$\alpha = 3\mathrm{II}_{(002)}/\left(3\mathrm{II}_{(002)} + \mathrm{II}_{(200)}\right) \quad (1)$$

where, $II_{(002)}$ and $II_{(200)}$ are integrated XRD intensities of (002) and (200) diffraction peaks, respectively.

From the variation of α with reaction time, the formation rate of tetragonal $BaTiO_3$ phase was investigated by using of Johnson-Mehl-Avrami equation. Seo *et al.* applied this method to interpret the kinetics for the hydrothermal crystallization of cubic $BaTiO_3$ powder [5].

The Johnson-Mehl-Avrami equation in linear form is;

$$\ln[-\ln(1-\alpha)] = \ln(r) + m\ln(t) \qquad (2)$$

where α, fractional yield of the tetragonal phase at time t; r, a constant that partially depends on nucleation frequency and rate of grain growth; m, a constant that varies with the system geometry.

A preliminary examination of the sintering characteristics of the $BaTiO_3$ powder was performed. The powders were compacted uniaxially in a stainless steel die (pressure $\approx$ 50 MPa) followed by cold isostatic pressing under a pressure of 250 MPa to produce pellets (20 mm in diameter by 5 mm) with a green density of 0.65 of the theoretical value. The compacts were sintered in air for 1 h at a constant heating rate of 10°C/min to 1350°C. For electrical characterization of the prepared samples, the samples were polished, and electrodes were deposited on both faces by silver paste (DS-7178RT, Daejoo Chem. Co., Korea) through a metallic screen. The electrodes were annealed at 400°C for 30 min to burn off the organic binder, then 750°C for 30 min. The relative dielectric constant was measured between room temperature and 200°C by LCR-meter (HP-4280, 1 kHz).

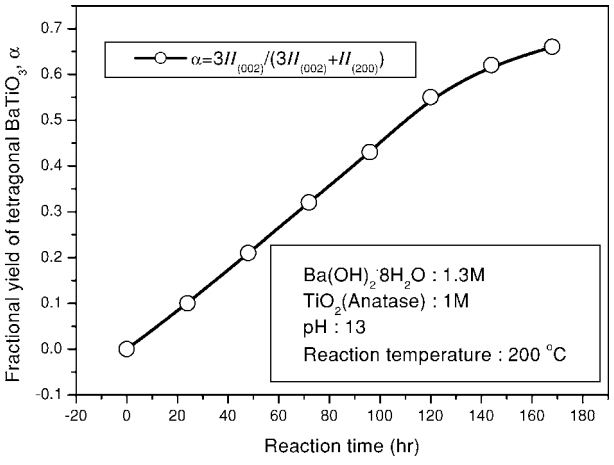

Figure 1 Fractional yield of product tetragonal $BaTiO_3$ powder as a function of reaction period at 200°C (with agitation (470 rpm), 1.3 M $Ba(OH)_2{\cdot}8H_2O$, 1 M TiO_2(Anatase) and pH 13).

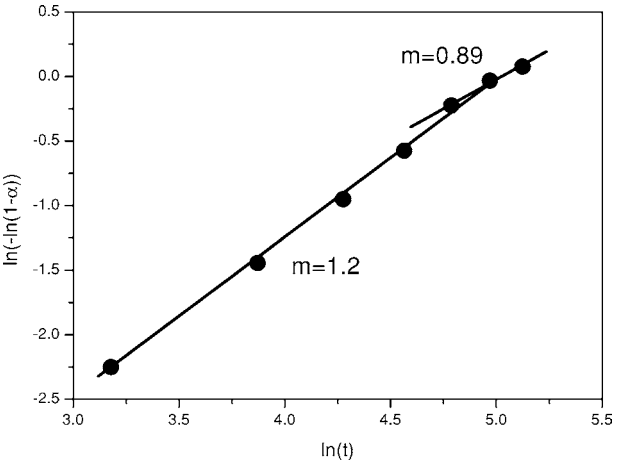

Figure 2 Plot based on the Johnson-Mehl-Avrami analysis of the experimental data shown in Fig. 1; a = fraction of tetragonal phase in $BaTiO_3$ powder, m = system geometry, t = time (h).

3. Results and discussion

It has been reported that hydrothermal $BaTiO_3$ powder is cubic form and its tetragonality increases as the reaction time and pH increases [7, 10, 11]. Calcination of synthesized cubic $BaTiO_3$ powder is another effective route to enhance its tetragonality. Hence, in the present study, pH of the solution and reaction temperature were fixed at 13 and 200°C respectively, then the formation rate of tetragonal $BaTiO_3$ phase was investigated as a function of reaction time. Before the measurement of the tetragonal phase, all the synthesized powders were calcined at 1200°C for 3 h which had been found from preliminary experiments to be optimum conditions. Fig. 1 shows the fractional yield of tetragonal $BaTiO_3$ calculated by Equation 2 as a function of reaction period at 200°C. The synthesized $BaTiO_3$ particle with 24 h of reaction time keeps mostly its cubic structure in spite of calcinations at 1200°C for 3 h, and only 10% of tetragonal phase was found in the calcined powder by XRD analysis. The tetragonal phase linearly increased as the reaction time increased up to 120 h and then it slightly decreased. Finally 66% of tetragonal phase was obtained at 168 h of reaction. The fraction yield (α) data shown in Fig. 1 was rearranged by Johnson-Mehl-Avrami equation. A plot of $\ln[-\ln(1-\alpha)]$ against $\ln(t)$ over $\alpha = 0.1$–0.66 is shown in Fig. 2. It was calculated that $m = 1.2$ until 100 h of reaction time and it changed to 0.9 from 120 h. Seo reported the reaction is controlled by grain boundary reaction at $m > 1$ in the hydrothermal synthesis of $BaTiO_3$, while it changes to diffusion control reaction at $m < 1$ [5]. The synthesis reaction rate of $BaTiO_3$ by hydrothermal process reaches nearly to 90% within 30 min at 180°C [11]. Here, m is observed to be over 1, which means the cubic $BaTiO_3$ phase is rapidly formed by dissolution and precipitation in hydrothermal condition. Also, it is certain that the formation reaction of tetragonal $BaTiO_3$ was controlled by diffusion through the long reaction time. It should be noted that the transformation to tetragonal phase from cubic $BaTiO_3$ was very difficult even by calcinations as shown in Fig. 1 although the particle size increased to over the critical particle size which is known to be from 49 [12] to 190 nm [13]. However, the particle size of $BaTiO_3$ before calcinations was approximately 200 nm, which means the cubic phase was not attributed to the size effect. Dutta reported that $BaTiO_3$ particle grows by the ripening of fine crystals during dissolution and precipitation [14]. In this mechanism, the cubic $BaTiO_3$ crystals precipitated in the early stage of the hydrothermal reaction agglomerated and formed sub-micron sized $BaTiO_3$ particle. The nano sized crystals were also observed

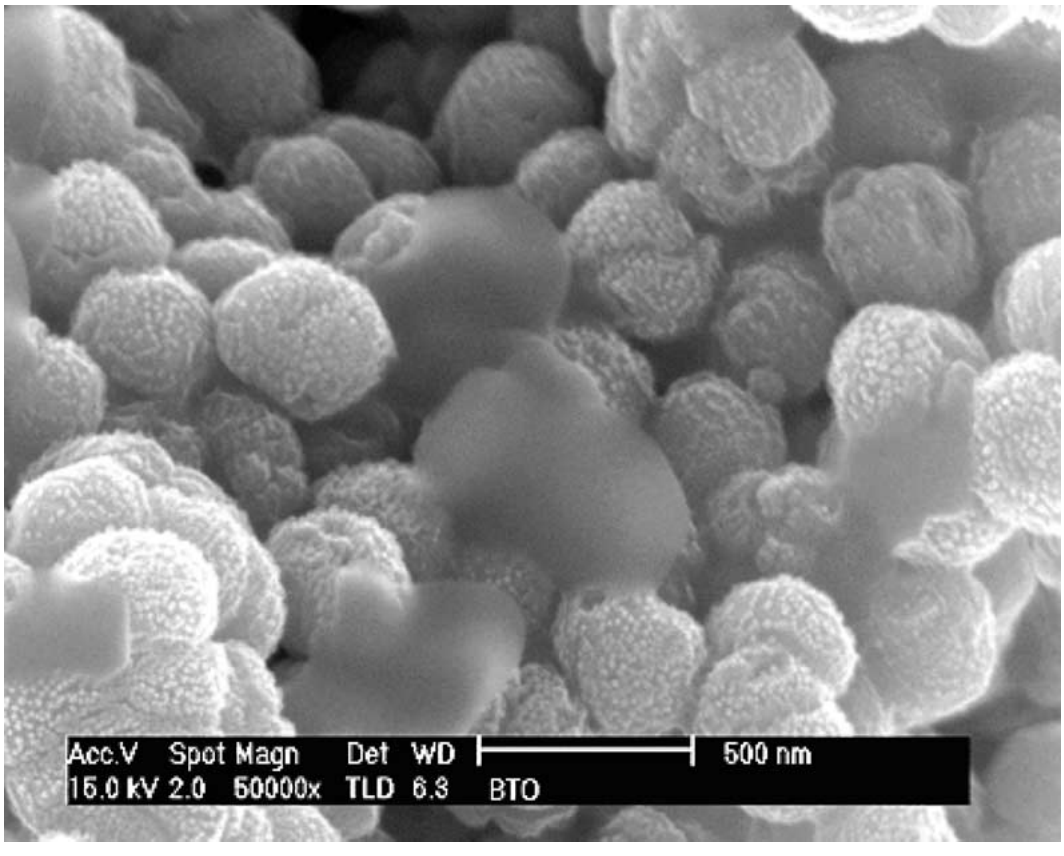

Figure 3 FESEM photograph of $BaTiO_3$ powder hydrothermal synthesized at 200°C for 3 h.

on the surface of the submicron size particle as shown in Fig. 3. Hence, the early stage of $BaTiO_3$ particle synthesized by the hydrothermal process seems to be the formation of aggregates composed of nano crystals of below critical crystal size; severe aggregation was found after the calcinations of the powders. From this result, we concluded that the surfaces of the nano particles were incorporated within the $BaTiO_3$ particle during calcination, acted as lattice defects then hindered the transformation to tetragonal phase. Also, the decrease of the tetragonal transformation rate at 120 h of reaction temperature may be attributed to the decrease of surface area and diffusion rate of Ba^{2+} to lattice by densification of the $BaTiO_3$ particle.

Fig. 4 shows X-ray diffraction traces with the 43 to 47 of 2θ range expanded in order to clearly define the (200) and (002) splitting for tetragonal phase. Without calcination, mainly the cubic phase with a small amount of tetragonal was obtained as shown in Fig. 4a. The peak splitting tendency increased as the calcination temperature increased and was most clearly shown in the condition of 1200°C for 3 h as shown in Fig. 4c. Hence, the calcination temperature was fixed to 1200°C and the peak splitting was analyzed by XRD as a function of calcination time. It can be seen that the splitting increased as the calcination time increased and then decreased after 5 h, see Fig. 5. The recombination of

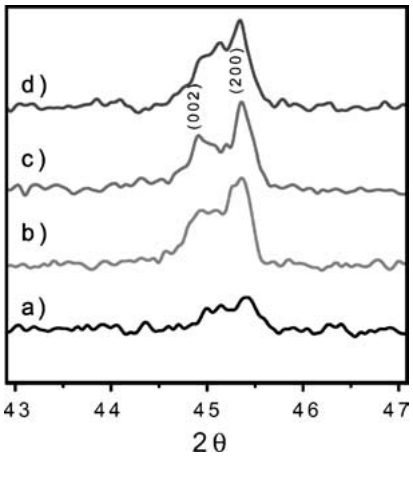

Figure 4 X-ray diffraction traces of the (200) and (002) reflections for $BaTiO_3$ powders with calcination temperature: (a) Before calcination, (b) 1100°C, 3 h, (c) 1200°C, 3 h, and (d) 1300°C, 3 h.

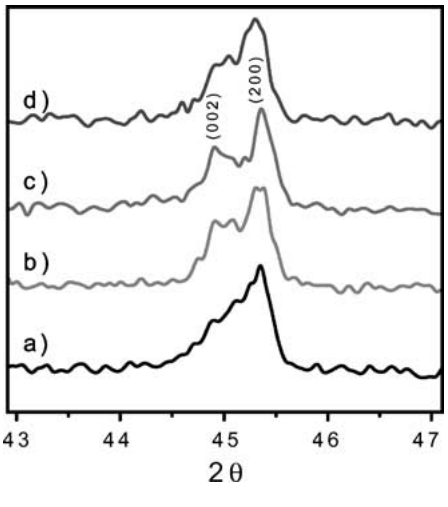

Figure 5 X-ray diffraction traces of the (200) and (002) reflections for $BaTiO_3$ powders with calcination time at 1200°C. (a) 1 h, (b) 2 h, (c) 3 h, and (c) 5 h.

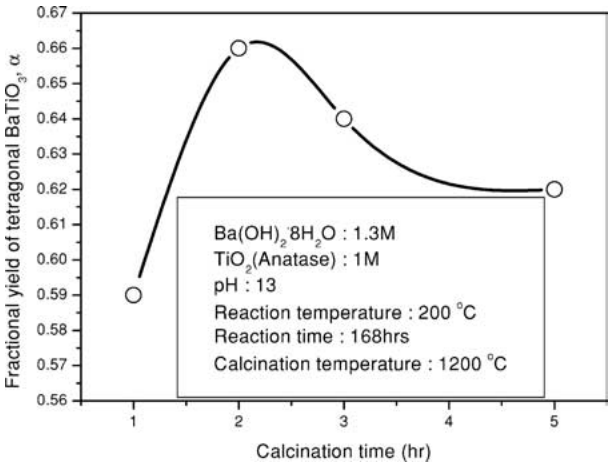

Figure 6 Fractional yield of tetragonal phase as a function of calcination time of hydrothermally synthesized $BaTiO_3$ powder.

(200) and (002) peak was found in the samples calcined at 1300°C for 3 h and 1200°C for 5 h as shown in Figs 4d and 5d respectively. The XRD patterns shown in Fig. 5 was rearranged by Equation 1. A plot of fraction yield (α) of tetragonal $BaTiO_3$ against calcination time is shown in Fig. 6. A maximum yield was found at 2 h of calcination time (Fig. 6). It has been reported that sintered $BaTiO_3$ ceramic are subjected to large elastic strains during the Curie transition, because grains in a ceramic are clamped by their neighboring grains, a slight unit-cell dimension change during the transition leads to large elastic strains within the cells. Such large strains cause the entire state to be unstable. Thus, it can be concluded that the decreases of the tetragonality were attributed to the constrained crystals having strain accumulated during crystal growth. The $BaTiO_3$ powders prepared by the hydrothermal method yielded a

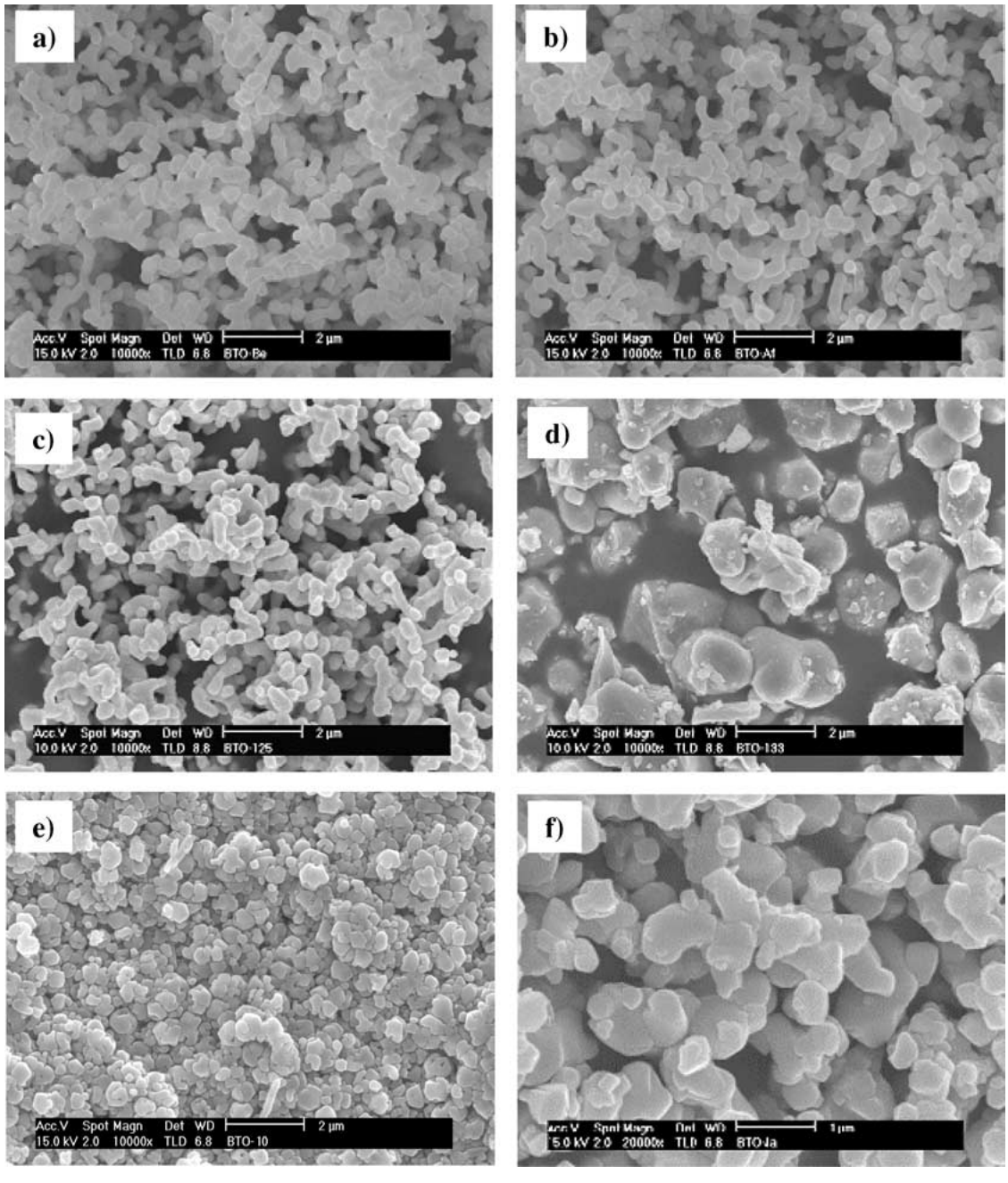

Figure 7 FESEM photographs of $BaTiO_3$ powders (a) hydrothermal synthesized at 200°C for 168 h and calcined at (b) 1200°C for 3 h, (c) 1200°C for 5 h, (d)1300°C for 3 h after hydrothermal synthesized at 200°C for 168 h, and (e) reagent grade powder.

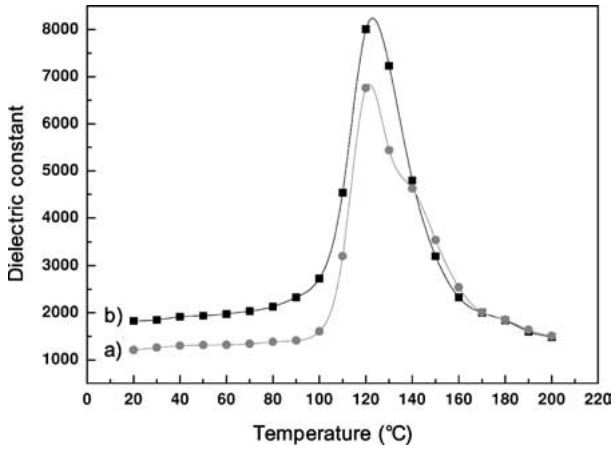

Figure 8 Temperature dependence of the dielectric constant of $BaTiO_3$ specimens sintered at 1350°C for 1 h: (a) reagent grade and (b) calcined at 1200°C for 3 h after hydrothermal synthesis.

particle size of about 0.5–0.7 μm with longish particle and uniform shape as shown in Fig. 7a. From the SEM micrographs, it is obvious that the particles were formed through dissolution and precipitation as well as ripening mechanism. Also, no significant changes in morphology were found in the sample calcined at 1200°C for 3 h, which show high tetragonality, as shown in Fig. 7b. In the case of the sample calcined at 1200°C for 5 h, Fig. 7c, the surface of the particle became rough and particles were somewhat longer. It was found that the particle size calcined at 1300°C for 3 h increased to around 2 μm with irregular particle shape and distribution. This abnormal particle growth may cause the $BaTiO_3$ particle to keep its cubic structure due to the internal strain as mentioned above. The reagent grade $BaTiO_3$ powder (Kojundo Chemical Lab. Co., LTD, Japan) synthesized by solid state reaction was presented in Fig. 7e for the comparison. The average particle size of the reagent grade $BaTiO_3$ powder is similar to the hydrothermal powder, while the particle shape is somewhat irregular.

The curve of dielectric constant is presented as a function of the temperature in Fig. 8 for the sample having highest tetragonality and reagent grade powder. The dielectric constant of the hydrothermal sample at room temperature reaches 1900, while 1100 for reagent grade sample. This value is reasonable compared to the reported for a pure $BaTiO_3$ ceramic obtained by conventional sintering. A dielectric constant of the hydrothermal sample at Curie temperature was measured to be 8000 while a dielectric constant of 6600 was observed for reagent grade $BaTiO_3$ ceramic at that temperature as shown in Fig. 8. The higher dielectric constant of hydrothermal $BaTiO_3$ ceramic is due to the homogeneous microstructure, i.e., monodispersed and uniform size distribution.

4. Conclusion

The hydrothermal processing of TiO_2 and $Ba(OH)_2 \cdot 8H_2O$ precursors leads to submicron sized tetragonal $BaTiO_3$ powders after calcination. The tetragonality of the powder increased as the hydrothermal reaction time increased and the formation reaction of tetragonal $BaTiO_3$ phase was controlled by diffusion for most of the reaction time. One of the most important observations is that $BaTiO_3$ powder synthesized at the early stage of hydrothermal reaction consists of aggregates of nano sized crystals, and a calcination of the powder didn't enhance its tetragonality probably due to abnormal crystal growth. The dielectric constant of the hydrothermal sample with 168 h of reaction time at Curie temperature was measured to be 8000, which is a relatively high value probably due to a monodispersed and uniform size distribution.

References

1. M. H. LEE, I. C. HWANG, W. K. CHOO and B. H. LEE, *J. Korean Ceram. Soc.* **15** (1978) 140.
2. D. VOLTZKE, H. P. ABICHT, E. PIPPEL and J. WOLTERSDORF, *J. European Ceram. Soc.* **20** (2000) 1663.
3. D. E. COLLINS and E. B. SLAMOVICH, *J. Mater. Res.* **15**(8) (2000) 1834.
4. M. Z. HU, V. KURIAN, E. A. PAYZANT, C. J. RAWN and R. D. HUNT, *Powder Technology* **110**(1/2) (2000) 2.
5. K. W. SEO and J. K. OH, *J. Ceram. Soc. Jpn.* **108**(8) (2000) 691.
6. S. W. LU, B. I. LEE, Z. L. WANG and W. D. SAMUELS, *J. Cryst. Grow.* **219** (2000) 269.
7. M. WU, J. LONG, G. WANG, A. HUANG and Y. LUO, *J. Amer. Ceram. Soc.* **82**(11) (1999) 3254.
8. J. H. LEE, C. W. WON, T. S. KIM and H. S. KIM, *J. Mater. Sci.* **35**(17) (2000) 4271.
9. C. LI, Z. CHEN, D. CUI, Y. ZHU, H. LU, C. DONG, F. WU and H. CHEN, *J. Appl. Phys.* **86** (1999) 4555.
10. E. CIFTCI, M. N. RAHAMAN and M. SHUMSKY, *J. Mater. Sci.* **36**(20) (2001) 4875.
11. R. ASIAIE, W. ZHU, S. A. AKBAR and P. K. DUTTA, *Chem. Mater.* **8**(1) (1996) 226.
12. S. SCHLAG and H. F. EICKE, *Solid State Commun.* **91**(11) (1994) 883.
13. B. D. BEGG, E. R. VANCE and J. NOWOTNY, *J. Amer. Ceram. Soc.* **77**(12) (1994) 3186.
14. P. K. DUTTA, R. ASIAIE, S. A. AKBAR and W. ZHU, *Chem. Mater.* **6**(9) (1994) 1542.

Received 1 May 2002
and accepted 4 September 2003